

Solid-liquid equilibrium and heat capacity trend in the alkylimidazolium PF₆ series



Paulo B.P. Serra ^{a,b}, Filipe M.S. Ribeiro ^a, Marisa A.A. Rocha ^a, Michal Fulem ^{b,*}, Květoslav Růžička ^b, João A.P. Coutinho ^c, Luís M.N.B.F. Santos ^{a,*}

^a CIQUP, Departamento de Química e Bioquímica, Faculdade de Ciências, Universidade do Porto, Rua do Campo Alegre, 687, P-4169-007 Porto, Portugal

^b Department of Physical Chemistry, University of Chemistry and Technology, Prague, CZ-166 28 Prague 6, Czech Republic

^c CICECO, Departamento de Química, Universidade de Aveiro, P-3810-193 Aveiro, Portugal

ARTICLE INFO

Article history:

Received 5 January 2017

Received in revised form 24 September 2017

Accepted 8 October 2017

Available online 14 October 2017

Keywords:

Drop calorimeter

Heat capacity

Imidazolium

Hexafluorophosphate

Ionic liquids

CAS

Nanostructuration

Odd-even effect

Thermal behavior

Glass transition

Melting: V shape

ABSTRACT

The heat capacity and thermal behavior trend along the 1-alkyl-3-methylimidazolium hexafluorophosphate [C_nC₁im][PF₆] (with n = 2–10, 12) ionic liquids series, is used to explore the effect of the alkyl chain length in the nanostructuration. The heat capacities of the studied ILs were measured with an uncertainty better than ± 0.15% and are in excellent agreement with the available data in the literature. An odd-even effect for the specific and volumic heat capacities of the [C_nC₁im][PF₆] series was found. The observed odd-even effect in the liquid heat capacity was rationalized considering the preferential orientation of the terminal —CH₃ group. The higher specific/volumic heat capacities shown for the [C₆C₁im][PF₆] and [C₈C₁im][PF₆] are an indication of an additional conformational disorder increase in the liquid phase that could be related with a weaker alkyl chain interdigitation capability of the even number chain ILs. The melting temperatures and consequent $\Delta_m^l H_m^0$ and $\Delta_m^l S_m^0$ trend along the alkyl series present a V-shape profile that is explained based on the analysis of the balance between the initial decrease of the electrostatic interaction potential and the increase of the van der Waals interactions with the increasing size of the alkyl side chain of the cation. The inhibition of crystallization for intermediate alkyl chain size (from [C₅C₁im][PF₆] to [C₈C₁im][PF₆]) seems to arise from the overlapping of the hypothetical cold crystallization temperature by the melting temperature. Above the critical alkyl size, CAS, a regular increase in the entropy and enthalpy profiles presents a similar shape than the observed in other alkane series and is a strong support of the intensification of the ILs nanostructuration.

© 2017 Elsevier B.V. All rights reserved.

1. Introduction

Ionic liquids, ILs, are known for possessing high viscosities, high heat capacities and high electrical conductivity, higher than the common organic solvents. All the ILs properties can be tuned by simply exchanging their components [1–5] as well by the change of the alkyl chain length in the cation or anion. This is an important feature for both science and industrial fields because the ILs can be easily adapted to different applications. The research on their physicochemical properties is of great importance for the better understanding of structure-property relationships between the different cation-anion combinations, allowing the design of new and improved ILs [5]. Some ILs are considered as nanostructured systems that tend to organize themselves into heterogeneous regions due to the separation of polar (head polar groups and anions) and non-polar domains (long alkyl chains), maximizing their electrostatic interactions and maintaining the electroneutrality

conditions of the cation/anion aggregation [6]. The transition between polar and non-polar domains was observed in different properties, when the effect of the alkyl chain length of the cation was investigated [7–9]. The effect of the nanostructuration in the ILs properties was found to be intensified at the denominated critical alkyl size, CAS typically at n = 6 [7–9].

In general, ILs exhibit relatively weak coulombic interactions compared to the molten salts, due to the charge delocalization of asymmetric ions [1–6]. This leads to an inefficient arrangement of the crystal lattice, and consequently, lower melting temperatures of ILs and in many cases, glass formation with marked inhibition of crystallization. These features lead to complex solid - liquid phase behavior [10–12]. For many ILs, the cooling of the liquid phase tends to pass to a metastable equilibrium (undercooling), and later to glass formation. In these cases, the kinetics of the crystallization, mainly governed by the liquid cooling rate, plays an important role. As a result, in order to obtain reliable thermal phase behavior data, long equilibration times and small samples are needed [13,14]. The main works reporting thermal phase behavior of ILs were performed using differential scanning calorimetry

* Corresponding authors.

E-mail addresses: fulemm@vscht.cz (M. Fulem), lbsantos@fc.up.pt (L.M.N.B.F. Santos).

(DSC). The obtained data for these systems have revealed multiple solid-solid transitions, e.g. crystal-crystal polymorphism, as detected for 1-butyl-3-methylimidazolium chloride ($[C_4C_1im][Cl]$) [11], and in some cases the ILs exhibit plastic-crystal transitions, which consumes a fraction of the energy of fusion leading to crystal - liquid transition with a lower enthalpy of fusion [15]. The existence of crystal polymorphism in the ILs indicates a level of a more complex structure [12] and also contributes for a differentiation on the thermophysical properties, such as, melting temperatures and heat capacities. Holbrey et al. [11] found the existence of two type of crystals in $[C_4C_1im][Cl]$ which differ only in the conformation of the alkyl chain. Later that work was complemented with the thermal behavior studies of the two crystalline forms by Nishikawa et al. [16].

The 1-alkyl-3-methylimidazolium hexafluorophosphate ILs series is one of the most studied series [17]. Gordon et al. [17] presented a compilation of phase transition temperatures for the imidazolium hexafluorophosphate series, $[C_nC_1im][PF_6]$ with long alkyl chains ($n > 12$), where it was found an increase of the melting temperatures along the alkyl chain. Later, Triolo et al. [18] reported a thermodynamic, structural, and dynamical information obtained for $[C_4C_1im][PF_6]$ in its amorphous glassy and liquid state, using quasi-adiabatic, continuous calorimetry, and X-ray and neutron scattering. Based on the results it was possible to observe that the studied IL show a considerable degree of order in their amorphous states, which resembles the crystalline order and a complex crystal polymorphism has been characterized [18]. Endo et al. [19–21] presented three individual studies about two $[PF_6]$ ILs, $[C_2C_1im][PF_6]$ [19] and $[C_4C_1im][PF_6]$ [20,21], where based on the thermal phase behavior complemented with Raman spectroscopy, they were able to distinguish different crystalline phases of both compounds, showing that polymorphism is a characteristic of ILs with short alkyl chain size. The different crystalline phases of $[C_4C_1im][PF_6]$ were detected with some difficulty since the solid-solid transition did not possess a fixed temperature and was dependent on the measurement heating rate [19]. This behavior was also described for $[C_4C_1im][PF_6]$, together with the detection of different crystalline phases. This last IL was the focus of study of many scientific groups, leading to well-known heat capacities [9,22,23].

Holbrey et al. [24] studied the phase behavior of an analogous series, $[C_nC_1im][BF_4]$ (for $n = 0–18$), where the T_m displayed a V-shaped trend. Their study showed that for intermediate alkyl chain size ($n = 2–9$) the ILs did not crystallize, undergoing a supercooled state or glass transition, remaining liquid down to a lower limit of 193 K. The remaining ILs (for $n = 0, 1$ and $n = 10–18$) do not present a linear trend when compiling the melting temperatures as function of the size of the alkyl chain. For low alkyl chain size, the $[BF_4]$ series presented a decrease in the melting temperature with the $—CH_2—$ increment, while for long alkyl chains, an increasing of the melting temperatures, per $—CH_2—$ group, was observed.

The V-shaped trend presented above [24] was later observed on physical properties studies for $[C_nC_1im][PF_6]$ and $[C_nC_1im][NTf_2]$ with $n = (2–10)$ as reported by Dzyuba et al. [25] and Rodrigues et al. [7].

More recently, the behavior observed for the T_m of the $[C_nC_1im][PF_6]$ series was reproduced by Zhang and Maginn [26] using molecular simulation studies. Before the CAS, the reason for the decrease in the T_m with the increasing alkyl chain length is mainly entropic. After the CAS, the dispersive interactions become dominant, leading to an increasing melting enthalpy per $—CH_2—$ increment and overcoming the melting entropy [26]. Nemoto et al. [27] presented another calorimetric study with T_g and T_m values. The values for pure compounds are in agreement with the trend mentioned above for $[BF_4]$ and $[PF_6]$. For long alkyl chains, ILs tend to present transitions from liquid to liquid-crystal, revealing the high level of organization in the liquid phase.

For other series, as for example for the $[NTf_2]$ series, the melting temperatures do not seem to follow any trend [7,28]. In this case, the cation size plays an important role, governing the packing system and diminishing the importance of short side alkyl chains [12]. For example,

Shimizu et al. [28] studied the dependence of thermodynamic properties on alkyl-chain-length also for an analogous series, $[C_nC_1im][NTf_2]$ (for $n = 2–18$), and concluded that the entropy of the crystalline state for members with short alkyl chain dominates their low melting points.

In this work, the thermal behavior (temperature range of 183 K to 423 K) of 1-alkyl-3-methylimidazolium hexafluorophosphate, $[C_nC_1im][PF_6]$ (with $n = 2–10, 12$), was measured by a differential scanning calorimeter (TA Q1000, TA Instruments, USA). The thermal behavior study was complemented with the heat capacities studies of each IL. The heat capacity data have a wide field of application in chemical engineering for establishing energy balances, in thermochemistry for calculating changes in reaction enthalpies as well as in evaluation of molecular and supramolecular interactions and structural changes of materials. Simultaneously, the phase behavior analysis complements the heat capacities studies, allowing the comprehension of existing molecular arrangements, most stable crystalline phases and consequently, other adjacent properties. The same samples used for thermal behavior studies were measured with a Tian-Calvet calorimeter in the temperature range of 258–353 K, for heat capacities studies and support the high-precision heat capacity drop calorimeter [29–31] results measured at $T = 298.15$ K. This work is part of a wider project related with the effect of nanostructuration on thermophysical properties of ILs [7,9,32–34].

The experimental results obtained for the molar, specific and volumic heat capacities and thermal behavior will be used to evaluate the effect of the nature and size of the anion, as well as the impact of the nanostructuration of ILs on the thermophysical properties. This analysis will be performed in a comparative basis with the literature data for the $[C_nC_1im][NTf_2]$ IL series [7].

2. Experimental details

2.1. Materials and purification

The 1-alkyl-3-methylimidazolium hexafluorophosphate, $[C_nC_1im][PF_6]$ (with $n = 2–10, 12$, Fig. 1), used in this work, were purchased from IOLITEC with a stated purity of better than 99% (additional information is listed as SI). The samples were distributed among the two laboratories, and independent purification processes were performed. All the ILs were purified and stored under vacuum (<10 Pa) at moderate temperature (room temperature to 323 K) and constant stirring, to reduce the presence of water or other volatile contents. This process was performed systematically before the thermophysical properties measurements. The low content of water (<500 ppm) was measured and confirmed by Karl-Fischer titration.

2.2. Phase behavior measurements

The phase behavior of the studied ILs was explored in the temperature range of 183 K to 423 K with a differential scanning calorimeter (TA Q1000, TA Instruments, USA) using the continuous method with a heating rate of 5 K min^{-1} and sealed aluminum crucibles. The temperature and heat flux scales of the calorimeter were calibrated using water, gallium, naphthalene, indium, and tin.

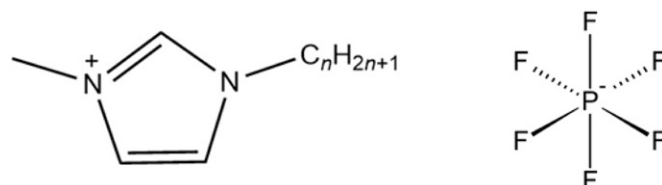


Fig. 1. Schematic representation of the 1-alkyl-3-methylimidazolium cations, $[C_nC_1im]^+$, and the studied anion, hexafluorophosphate $[PF_6]^-$. The size of the alkyl chain from $n = 2–10$ and 12.

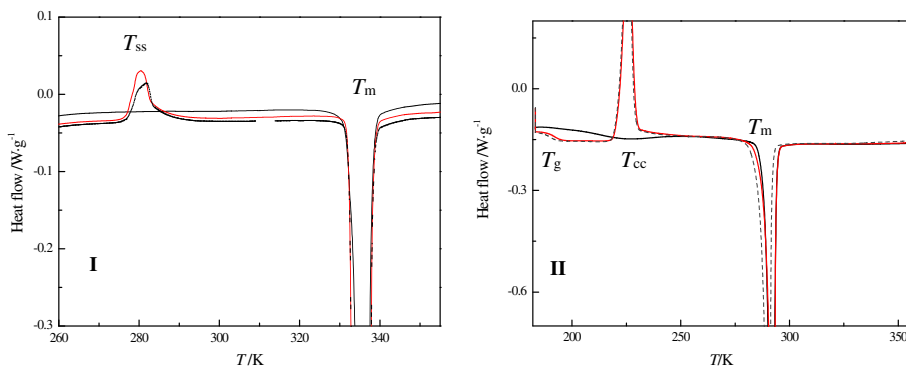


Fig. 2. Typical thermograms obtained by DSC using the described experimental methodology: (I) - $[C_2C_1\text{im}][\text{PF}_6]$, solid-solid relaxation transition T_{ss} was found 30 to 50 K before the melting temperature (at 0.3 K min^{-1}); (II) - DSC thermogram for $[C_{10}C_1\text{im}][\text{PF}_6]$. Exhibiting the glass transition after the first melting cycle, followed by a cold crystallization and melting. Black, red, and dashed lines represent the first, second, and third consecutive DSC temperature scans (5 K min^{-1} heating rate).

Table 1

Experimental glass, T_g , solid-solid, T_{ss} , cold crystallization T_{cc} , and melting temperatures, T_m , are presented together with the T_g/T_m ratio for the $[C_n\text{mim}][\text{PF}_6]$ series ($n = 2-10, 12$).

Ionic liquid	T_g/K	T_{ss}/K	T_{cc}/K	T_m/K	T_g/T_m
$[C_1C_1\text{im}][\text{PF}_6]$	–	–	–	(α , 364.3) ^a (β , 314.3) ^a	–
$[C_2C_1\text{im}][\text{PF}_6]$	–	279.4 ± 0.8	$(297 \pm 1)^b$	334.2 ± 0.3 $(333 \pm 1)^b, (332.8 \pm 1)^c$, $(331.1 \pm 4)^d, (334.1 \pm 1)^e$, $(335 \pm 2)^f, (333 \pm 3)^g, (341-343)^o, (335.7)^p, (335)^q$	–
$[C_3C_1\text{im}][\text{PF}_6]$	$(199.2)^d$	–	219.1 ± 0.3	311.8 ± 0.3 $(294.2^d, 310-312)^o$	–
$[C_4C_1\text{im}][\text{PF}_6]$	196.0 ± 0.9 $(196.2^d, 190.6^h$, $196.2^l, 194.0^l, 195^p, 194^r, 193^s, 196^t)$	–	(226.5^d)	$(276.4^c, 283.5^h$, $283 \pm 6^i, 282.3^j$ $284 \pm 1^k, 283 \pm 2^l$ $\gamma = 285.3 \pm 0.7^m$ $\beta = 285.8 \pm 0.7^m, 281.8^n, 285^u, 283^v, 278^w$)	0.687
$[C_5C_1\text{im}][\text{PF}_6]$	199.2 ± 1.2 $(193.2^d, 197^p)$	–	–	–	–
$[C_6C_1\text{im}][\text{PF}_6]$	201.7 ± 0.4 $(193.2^d, 197.4^j, 199^p)$	–	–	–	–
$[C_7C_1\text{im}][\text{PF}_6]$	203.5 ± 0.5 $(189.2^d, 201^p)$	–	–	–	–
$[C_8C_1\text{im}][\text{PF}_6]$	203.5 ± 0.4 $(202.2^d, 199.8^j)$	–	–	267.3 ± 0.3 (272.3^j)	0.761
$[C_9C_1\text{im}][\text{PF}_6]$	205.9 ± 0.3 $(207.2^d, 200.6^j)$	–	252.8 ± 0.5	293.0 ± 0.3 (287.1 ± 2^d)	0.703
$[C_{10}C_1\text{im}][\text{PF}_6]$	208.2 ± 0.3 $(202.2^d, 205.9^j)$	–	238.8 ± 0.8	307.1 ± 0.3 $(305.2 \pm 2^d, 308.4^j)$	0.678
$[C_{12}C_1\text{im}][\text{PF}_6]$	–	–	–	326.5 ± 0.3 (326.2^j)	–

Standard pressure ($p^0 = 10^5 \text{ Pa}$). Standard uncertainties, u , are $u(T) = 0.02 \text{ K}$, the 0.95 confidence level ($k \approx 2$).

- ^a Endo et al. [19].
- ^b Vila et al. [44].
- ^c Domanska et al. [45].
- ^d Dzyuba et al. [25].
- ^e Sifaoui et al. [46].
- ^f Ngo et al. [47].
- ^g Wong et al. [48].
- ^h Kabo et al. [23].
- ⁱ Tokuda et al. [49].
- ^j Nemoto et al. [27].
- ^k Fredlake et al. [50].
- ^l Huddlestone et al. [51].
- ^m Endo et al. [20].
- ⁿ Zhang et al. [52].
- ^o Talaty et al. [53].
- ^p Strehmel et al. [54].
- ^q Urahata et al. [55].
- ^r Shamim et al. [56].
- ^s Branco et al. [57].
- ^t Xu et al. [58].
- ^u Holopainen et al. [59].
- ^v Flieger et al. [60].
- ^w Su et al. [61].

Table 2

Experimental melting temperatures, T_m , and the respective enthalpies of melting, $\Delta_{cr}^l H_m^o$ and entropies of melting, $\Delta_{cr}^l S_m^o$.

Compound	T_m / K	$\Delta_{cr}^l H_m^o$ / kJ mol ⁻¹	$\Delta_{cr}^l S_m^o$ / J mol ⁻¹
[C ₁ C ₁ im][PF ₆]	–	(17.2 ^a)	(47.6 ^a)
[C ₂ C ₁ im][PF ₆]	334.2 ± 0.3	17.7 ± 0.1 (17.9 ^b ; 18.0 ^c ; 17.9 ^d)	53.2 ± 0.1
[C ₃ C ₁ im][PF ₆]	311.8 ± 0.3	14.1 ± 0.9	45.2 ± 1.0
[C ₄ C ₁ im][PF ₆]	–	(22.6 ^e ; 9.2 ^d , 19.9 ^e , 20.9 ^f , 20.7 ^g , 19.6 ^h)	(45.9 ^e , 73.3 ^f)
[C ₈ C ₁ im][PF ₆]	–	(12.9 ^g)	(47.0 ^g)
[C ₉ C ₁ im][PF ₆]	293.0 ± 0.3	16.5 ± 0.1	56.4 ± 0.2
[C ₁₀ C ₁ im][PF ₆]	307.1 ± 0.3	19.4 ± 0.5 (21.7 ^f)	63.3 ± 1.7 (69.1 ^f)
[C ₁₂ C ₁ im][PF ₆]	326.5 ± 0.3	24.5 ± 0.2 (27.2 ^f)	75.2 ± 0.7

Standard pressure ($p^0 = 10^5$ Pa). Standard uncertainties, u , are $u(T) = 0.02$ K, the 0.95 confidence level ($k \approx 2$).

- ^a Endo et al. [19].
- ^b Sifaoui et al. [46].
- ^c Endo et al. [20].
- ^d Domanska et al. [45].
- ^e Troncoso et al. [75].
- ^f Zhang et al. [52].
- ^g Nemoto et al. [27].
- ^h Kabo et al. [23].

In order to reach a better differential analysis of the thermal behavior we follow the same experimental methodology and procedure used in a recent work [7]. During the thermal analysis of the ILs, two isotherms, one at the beginning and another at the end of each measurement, were performed to ensure the sample stabilization and remove the memory effect. In the first run, the initial isotherm was performed at 183 K, with a fast cooling, to observe the initial crystalline phase before the first melting, followed by the standard 5 K min⁻¹ heating, and the final isotherm at 400 K to ensure sample melting and stabilization. After the measurement, a final fast cooling down to 183 K, to induce possible amorphous state, was performed. The crucibles were weighted on a Denver Instrument analytical balance with a readability of 0.01 mg and the typical sample load was of about 10 mg. The handling of the ILs was performed in a glove box under nitrogen atmosphere.

2.3. Heat capacities measurements

2.3.1. Tian-Calvet type calorimetry

The heat capacities of condensed phases were measured with a Tian-Calvet type calorimeter (SETARAM model μDSCIIIa) in the range from 258 to 353 K using the incremental temperature step mode method [35]. Each 5 K step included a heating rate of 0.3 K min⁻¹ followed by an isothermal delay of 2600 s. The combined expanded uncertainty of the heat capacity measurements is estimated to be U_c ($C_{p,m}$) = $0.01 \cdot C_{p,m}$. A detailed description of the calorimeter and its calibration can be found in the literature [36]; the measuring procedure was described in detail in the reference [37].

2.3.2. High-precision heat capacity drop calorimetry

The heat capacities of the liquid [C_nC₁im][PF₆] (with $n = 4\text{--}9$) were measured at $T = 298.15$ K, by a high-precision heat capacity drop calorimeter, which is described in detail in the literature [29–31]. The calorimeter was calibrated with water and sapphire (α -Al₂O₃ pellets, NIST-RM 720) based on a drop temperature step procedure of $\Delta T = 10$ K [9, 22, 29–34, 38–40], using the respective standard molar heat capacities at 298.15 K reported in literature, $C_{p,m}^o(\alpha\text{-Al}_2\text{O}_3) = (79.03 \pm 0.08)$ J K⁻¹ mol⁻¹ and $C_{p,m}^o(\text{H}_2\text{O}) = (75.32 \pm 0.01)$ J K⁻¹ mol⁻¹ [41]. The calibration constant was found to be $\varepsilon = (6.6040 \pm 0.0036)$ W V⁻¹. The accuracy of the apparatus for the measurements of the heat capacities of liquids and solids was evaluated based on the measurements of benzoic acid and hexafluorobenzene [31]. It was additionally tested for ionic liquid samples with 1-hexyl-3-methylimidazolium bis(trifluoromethylsulfonyl)imide, [C₆C₁im][NTf₂]. The determined $C_{p,m}^o$ ([C₆C₁im][NTf₂], 298.15 K) = (629.24 ± 0.43) J K⁻¹ mol⁻¹ is in excellent agreement with the available literature data $C_{p,m}^o$ ([C₆mim][NTf₂], 298.15 K) = (631.6 ± 0.5) J K⁻¹ mol⁻¹ [38]. The calorimeter and the

same methodology was already used in the measurement of heat capacities for the imidazolium based IL series [38]. The obtained results differ < 0.4% from the literature data, in excellent agreement with the best heat capacity data obtained by high precision adiabatic calorimetry [42]. The mass of the ILs samples and calibration compounds were corrected for the buoyancy effect. The relative atomic masses used were those recommended by the IUPAC Commission in 2007 [43]. The presented uncertainties are presented as twice the standard deviation of the mean and the calibration uncertainty is included.

3. Results and discussion

3.1. Phase behavior

The thermal behavior of the studied ILs was evaluated by differential scanning calorimetry. The typical behavior for the studied ILs is presented in Fig. 2. The thermograms of the studied ILs are available as supporting information. The melting temperatures (T_m) were taken as the onset temperatures of the endothermic peak on heating, the cold crystallization temperature (T_{cc}) and the solid-solid transition temperatures (T_{ss}) were taken as the onset temperature of an exothermic peak on heating. The glass transition temperature (T_g) was taken as the midpoint of the heat capacity change on heating from the glass to a liquid transition. The T_g , T_{ss} , T_{cc} , T_m , and the T_g/T_m ratio for each of the studied ILs are presented in Table 1.

[C₂C₁im][PF₆] presents a T_{ss} that is dependent of the heating rate, not being detectable for fast heating rates. For low heating rates, it can be observed in a 20 K temperature interval (e.g. 270 K at 0.3 K min⁻¹). This phenomenon is due to differences in the crystal packing or from

Table 3

Experimental Δc_p values of the previously described phase transitions: T_g , T_{cc} and T_m .

Compound	$\Delta_g^l c_m$ / J K ⁻¹ g ⁻¹	$\Delta_{cr}^l c_p$ / J K ⁻¹ g ⁻¹	$\Delta_{cr}^l c_p$ / J K ⁻¹ g ⁻¹
[C ₂ C ₁ im][PF ₆]	–	–	0.09
[C ₃ C ₁ im][PF ₆]	(0.12 ^a)	–0.14	0.18
[C ₄ C ₁ im][PF ₆]	0.28 (0.18 ^a , 0.28 ^b)	–	–
[C ₅ C ₁ im][PF ₆]	0.34 (0.16 ^a)	–	–
[C ₆ C ₁ im][PF ₆]	0.39 (0.13 ^a , 0.26 ^b)	–	–
[C ₇ C ₁ im][PF ₆]	0.24 (0.23 ^a)	–	–
[C ₈ C ₁ im][PF ₆]	0.24 (0.07 ^a , 0.26 ^b)	–	–
[C ₉ C ₁ im][PF ₆]	0.23 (0.02 ^a , 0.26 ^b)	–0.25	0.28
[C ₁₀ C ₁ im][PF ₆]	0.29 (0.14 ^a , 0.29 ^b)	–0.28	0.27
[C ₁₂ C ₁ im][PF ₆]	–	–	0.29

Standard pressure ($p^0 = 10^5$ Pa). Standard uncertainties, u , are $u(T) = 0.02$ K, the 0.95 confidence level ($k \approx 2$).

- ^a Dzyuba et al. [25].
- ^b Nemoto et al. [27].

Table 4Fitted parameters, a , and b of Eq. (1).^a

Compound	Phase	$T_{\text{range}}/\text{K}$	$a/(\text{J K}^{-1} \text{ mol}^{-1})$	$b/(\text{J K}^{-2} \text{ mol}^{-1})$	$S_r/\%$ ^a
[C ₂ C ₁ im][PF ₆]	Crystal I	260–274	16.21	1.0335	0.54
	Crystal II	280–300	–48.41	1.2676	0.55
[C ₃ C ₁ im][PF ₆]	Liquid	340–355	200.77	0.4842	0.29
	Crystal	259–294	–10.11	1.2712	0.52
[C ₄ C ₁ im][PF ₆]	Liquid	265–345	242.21	0.5559	0.29
	Liquid	258–355	256.83	0.6055	0.20
[C ₅ C ₁ im][PF ₆]	Liquid	258–355	288.22	0.6062	0.24
[C ₆ C ₁ im][PF ₆]	Liquid	264–345	311.92	0.6329	0.24
[C ₇ C ₁ im][PF ₆]	Liquid	263–355	332.17	0.6839	0.12
[C ₈ C ₁ im][PF ₆]	Liquid	259–355	356.14	0.7153	0.09
[C ₁₀ C ₁ im][PF ₆]	Crystal	258–279	215.72	1.1174	0.01
	Liquid	314–355	387.93	0.7225	0.09
[C ₁₂ C ₁ im][PF ₆]	Crystal	283–294	172.98	1.5508	0.07
	Liquid	334–355	408.67	0.8763	0.06

^a $S_r = 100 \times \left\{ \sum_{i=1}^n \frac{[(C_p - C_p^{\text{calc}})/C_p^{\text{calc}}]^2}{n-m} \right\}^{1/2}$, where n is the number of fitted data points, and m is the number of independent adjustable parameters. Standard pressure ($p^0 = 10^5 \text{ Pa}$). Standard uncertainties, u , are $u(T) = 0.02 \text{ K}$, the 0.95 confidence level ($k \approx 2$).

the capability, of both cation and anion, to adopt more than one conformation in the crystal [62]. ILs with low alkyl chain lengths show higher tendency to exhibit polymorphic forms as mentioned in the introduction [11,63]. The [C₃C₁im][PF₆] presents a cold crystallization, only detectable for low heating rates (0.3 K min⁻¹). Increasing the alkyl side chain length, in the region from [C₄C₁im][PF₆] until [C₈C₁im][PF₆], only the glass transition was detected, being a consequence of the weakening of the electrostatic interactions and decrease of the cation symmetry. The melting temperatures of three polymorphic crystals of [C₄C₁im][PF₆] ILs was already reported in the literature [20], however in the present work we were not successful to achieve the crystallization of our sample. This can be a result of the ILs complex structuration, which promotes the formation of a non-organized glass state at low temperatures, as reported by other groups [7,58,64]. The graphic representation of the T_g , T_{ss} , T_{cc} and T_m values as a function of the number of carbon atoms in the alkyl side chains of the cation, n , for [C_nC₁im][PF₆] series, together with the available literature data, are depicted in Fig. 3.

The observed trend in the melting temperatures for the studied ILs is in good agreement with the reported trends in the literature [27]. A similar V-shape profile is found for the enthalpies and entropies of melting with the increasing alkyl chain length of the cation (Table 2 and Fig. 4), reflecting the an entropic-enthalpic compensation behavior [26].

The initial decrease in the melting temperatures (along the alkyl chain) is in agreement with the combination of the expected decrease of the electrostatic interactions and increase (linear) of the van der Waals interaction per —CH₂— group [65]. In addition, the loss of

symmetry of the cation contributes as well as, to a decrease of the melting temperature reaching a region where only glass transition is detected.

After the critical alkyl size, CAS typically at $n = 6$ [6,9,22], the increase of the alkyl chain does not significantly change the polar network (anion-cation) interaction and the structural organization of the ILs in the crystal. At this point, there is an intensification of the ILs structuration into two distinct regions: one polar region, mainly dominated by the cation-anion network interactions, and another non-polar segregated region (alkane-like domain) with essentially/predominant van der Waals interactions. In the non-polar region, the alkyl chain folding leads to an increase of the stability of the crystalline phase interaction that is growing continuously with the alkyl chain length. This is in agreement with the observed trends for long chain alkane derivatives [66–71] and the recent findings for the thermal behavior of [C_nC₁im][NTf₂] and [C_nC_nim][NTf₂] series [7].

The V-shape profile of the melting temperatures along the increase of the alkyl chain length is the result of effect of the combination of the change of the two interaction potentials in the crystalline and liquid phases that will be discussed and analysed considering the enthalpic and entropic trend along the series. The observed T_{cc} values (~200–270 K) are typically the temperatures associated in the alkanes and alkane derivatives to thermal motion needed to the alkyl group rotation [72,73]. The compiled T_{cc} follows a trend that goes in the opposite direction of the T_m and leads to the inability of the intermediate alkyl chain size compounds to form crystalline solids, since there would be

Table 5Liquid phase heat capacities at $T = 298.15 \text{ K}$.

Ionic liquid	$C_p^o/\text{J K}^{-1} \text{ g}^{-1}$	$C_p^o/\text{V J K}^{-1} \text{ cm}^{-3}$	$C_{p,m}^o/\text{J K}^{-1} \text{ mol}^{-1}$	$C_p^o/\text{J K}^{-1} \text{ g}^{-1}$	$C_p^o/\text{V J K}^{-1} \text{ cm}^{-3}$	$C_{p,m}^o/\text{J K}^{-1} \text{ mol}^{-1}$	$C_{p,m}^o/\text{J K}^{-1} \text{ mol}^{-1}$	$C_{p,m}^o/\text{J K}^{-1} \text{ mol}^{-1}$
μDSC IIIa microcalorimeter				Drop calorimeter			Literature	GCM [81]
[C ₂ C ₁ im][PF ₆]	1.348 ^a ± 0.014		345.1 ^a ± 3.5					343.6
[C ₃ C ₁ im][PF ₆]	1.386 ^a ± 0.014		374.4 ^a ± 3.7					375.6
[C ₄ C ₁ im][PF ₆]	1.436 ± 0.014	1.964 ± 0.020	408.0 ± 4.1	1.4310 ± 0.0018	1.9567 ± 0.0025	406.68 ± 0.51	408.7 ± 1.6 (AC) [23]	407.6
							407.7 ± 2.5 (TC) [75]	
							405 ± 12 (TC) ^b [82]	
[C ₅ C ₁ im][PF ₆]	1.467 ± 0.015	1.948 ± 0.020	437.4 ± 4.4	1.4603 ± 0.0021	1.9390 ± 0.0028	435.49 ± 0.63		439.6
[C ₆ C ₁ im][PF ₆]	1.503 ± 0.015	1.946 ± 0.020	469.0 ± 4.7	1.5012 ± 0.0017	1.9429 ± 0.0022	468.73 ± 0.54		471.6
[C ₇ C ₁ im][PF ₆]	1.535 ± 0.015	1.939 ± 0.019	500.6 ± 5.0	1.5350 ± 0.0016	1.9381 ± 0.0020	500.81 ± 0.52		503.6
[C ₈ C ₁ im][PF ₆]	1.576 ± 0.016	1.949 ± 0.020	536.1 ± 5.4	1.5727 ± 0.0016	1.9453 ± 0.0020	535.16 ± 0.56		535.6
[C ₉ C ₁ im][PF ₆]	1.608 ± 0.016	1.949 ± 0.020	569.4 ± 5.7	1.6000 ± 0.0013	1.9410 ± 0.0016	566.89 ± 0.45		567.6
[C ₁₀ C ₁ im][PF ₆]	1.639 ^a ± 0.016		603.3 ^a ± 6.0					599.6
[C ₁₂ C ₁ im][PF ₆]	1.690 ^a ± 0.017		666.3 ^a ± 6.7					663.6

Note: AC – adiabatic calorimetry; TC – Tian-Calvet microcalorimetry.

GCM – Gardas & Coutinho [81] group contribution method estimation. Standard pressure ($p^0 = 10^5 \text{ Pa}$). Standard uncertainties, u , are $u(T) = 0.02 \text{ K}$, the 0.95 confidence level ($k \approx 2$).^a The heat capacities of liquid phase were extrapolated to $T = 298.15 \text{ K}$.^b The heat capacity of [C₄C₁im][PF₆] was extrapolated to $T = 298.15 \text{ K}$ [81].

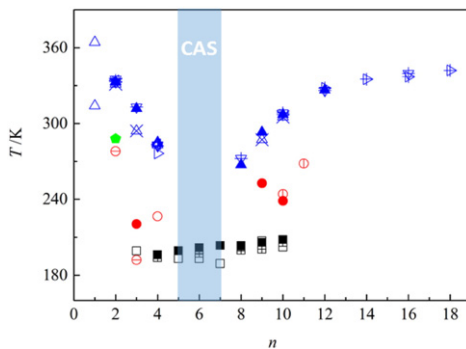


Fig. 3. Thermal behavior temperatures as function of the number of carbon atoms in the alkyl side chain of the cation, n , for $[C_nC_1\text{im}][\text{PF}_6]$ (with $n = 2-10, 12$). black symbols, T_g ; red symbols, T_{cc} ; green symbols, T_{ss} ; blue symbols, T_m – data obtained in this work. The available literature data are plotted as empty symbols (black for T_g , blue for T_m and red for T_{cc}). \triangle , Endo et al. [19]; \triangle , Endo et al. [20]; \diamond , López -Martin et al. [74]; \triangleright , Domanska et al. [45]; \triangledown , Troncoso et al. [75]; \blacktriangleleft , Sifaoui et al. [46]; \blacktriangleleft , Vila et al. [44]; \square , Dzyuba et al. [25]; \triangledown , \ominus , Ngo et al. [47]; \triangleright , Wong et al. [48]; \triangleleft , Kabo et al. [23]; \triangle , Tokuda et al. [49]; \blacktriangle , Fredlake et al. [50]; \triangleright , Huddlestone et al. [51]; \blacksquare , \ominus , Nemoto et al. et al. [27].

an overlay of T_{cc} and T_m . This agrees with the observed thermal behavior where the cold crystallization was not detected.

For the ILs with the shorter alkyl chain length, a decrease in the enthalpies of melting is observed, in agreement with already mentioned increase of the hindering effect which leads to a decrease of the localized electrostatic interaction. It is interesting to note that the entropy contribution per methylene group, $-\text{CH}_2-$, is small compared to the observed for the ionic liquids with long alkyl chains, indicating a very small perturbation in the solid-liquid entropy change with the increase of the alkyl chain length (but still in agreement to a molten salt-like melting). Above the critical alkyl size, CAS, a regular increase in the entropy and enthalpy profiles is observed with a similar shape observed in other alkane series [76,77]. The similarity of the shape and magnitude of the enthalpy and entropy increase per $-\text{CH}_2-$ group with the one observed in the alkane series [76,78] is a strong support/evidence of the existence of nanostructuration in the ILs, where the alkyl side chains segregates from the rest of the IL, forming a alkane-like domain separated from the polar network [79]. The detailed experimental results of the melting are presented in supporting information.

The graphic representation of the $\Delta_s^l H_m^0$ and $\Delta_s^l S_m^0$ as a function of the number of carbon atoms in the alkyl side chains of the cation, n , for $[C_nC_1\text{im}][\text{PF}_6]$ series, together with the available literature data, are depicted in Fig. 4.

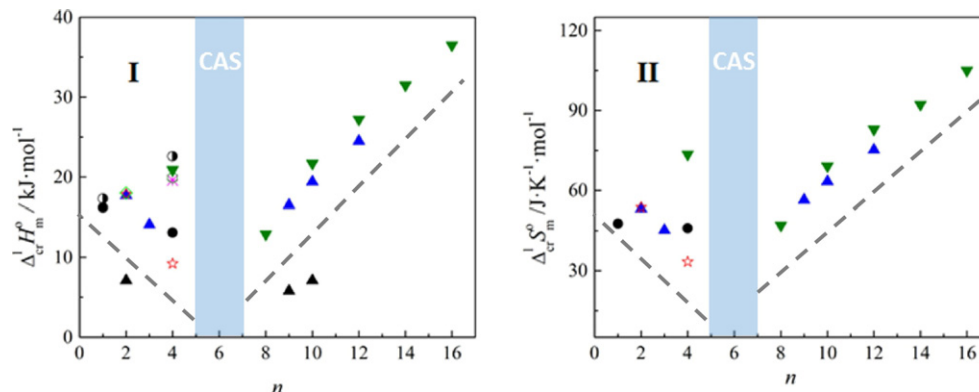


Fig. 4. Enthalpies (I) and entropies (II) of fusion as a function of the number of carbons in the alkyl side, n , chains of the cation, n , for $[C_nC_1\text{im}][\text{PF}_6]$ (with $n = 2-10, 12$). \blacktriangle , this work; \bullet , Endo et al. [19,20] (\bullet , γ form; \bullet , β form); \star , Domanska et al. [45]; \blacktriangle , Dzyuba et al. [25]; \circ , Troncoso et al. [75]; \times , Sifaoui et al. [46]; \blacktriangledown , Nemoto et al. [27]. Dashed lines are only view lines without any physical meaning.

The heat capacity change Δc_p associated for each phase transition was derived as the jump of heat capacity at the phase transition temperature (schematic description of the adopted methodology is presented as supporting information). The extrapolated onset temperature was adopted as a transition temperature and the difference in extrapolated signal to the transition point was regarded as Δc_p . The derived Δc_p data is presented in Table 3 and depicted in Fig. 5.

The heat capacity difference between the supercooled liquid and the glass at T_g shows a seems to present a gradual increase until $[C_6C_1\text{im}][\text{PF}_6]$, reaching a constant value around $\Delta_{cr}^{gl}c_p = 0.24 \text{ J K}^{-1} \text{ g}^{-1}$. This observation is in good agreement with previous works, where a trend shift at $n = 6$, the CAS, is detected in several physicochemical properties of ILs [7–9]. After CAS, a very small effect of the alkyl chain length in the heat capacity difference is observed.

3.2. Heat capacities

The heat capacities of all the ILs were measured using a Tian-Calvet differential type scanning calorimeter. The measurements were performed in the range from 258 to 353 K using the incremental temperature mode (step method) and measured at $T = 298.15$ K, by a non-commercial high-precision heat capacity drop calorimeter. The experimental heat capacities of the condensed phases obtained in this work are available as supporting information and are presented in Fig. 6.

In the experimental temperature range the experimental results could be quite well described, for each ionic liquid, by linear temperature dependence as follows:

$$C_{p,m} = a + b \cdot (T/K) \quad (1)$$

The fitted coefficients, a and b of Eq. (1) are listed in Table 4. The heat capacities of the liquid phase at $T = 298.15$ K obtained in this work together with the literature values are presented in Table 5. The molar heat capacity data predicted by the group contribution method (GCM) of Gardas and Coutinho [81] are also listed in Table 5 (at 298.15 K). It was found that the Gardas and Coutinho GCM could describe quite well the experimental data obtained in this work.

It was also found, an excellent linear correlation between the coefficients “ a ” and “ b ” of the Eq. (1) with the number of carbons in the alkyl chain “ n ” as described in Eqs. (2) and (3):

$$a/\left(\text{J} \cdot \text{K}^{-1} \cdot \text{mol}^{-1}\right) = 150.36 + 23.067 \cdot n \quad (2)$$

$$b/\left(\text{J} \cdot \text{K}^{-2} \cdot \text{mol}^{-1}\right) = 0.42719 + 0.030935 \cdot n \quad (3)$$

based on the linear fitting of “*a*” and “*b*” as function of “*n*” (*n* = 2 to *n* = 10). Eq. (4) was derived by analytical substitution of the coefficients “*a*” and “*b*” in Eq. (1),

$$C_{p,m}(n, T) / \text{J} \cdot \text{K}^{-1} \cdot \text{mol}^{-1} = 150.36 + 23.067n + 0.42719T + 0.030935n \cdot T \quad (4)$$

which describes the linear dependence of the molar heat capacities with (*n* and *T*) for the $[\text{C}_n\text{C}_1\text{im}]\text{[PF}_6]$ IL series, where, “*n*” is number of carbons in the alkyl chain of the and “*T*” the temperature in K. Eq. (4) was found to describes quite well (better than 1%) the molar heat capacity of the $[\text{C}_n\text{C}_1\text{im}]\text{[PF}_6]$ IL series in the “*n*” (*n* = 2 to 12) and “*T*” (253 to 355 K), as depicted in Fig. 7 which presents deviation plots of the experimental molar heat capacities from the model described in Eq. (4).

It is interesting to observe a “V” shape in the deviation plot that is centred in the *n* = 6 (CAS) and the good agreement of the experimental data with the Gardas and Coutinho [81] after the CAS number of *n* = 6.

Any heat capacity data was found in the literature for the ILs $[\text{C}_5\text{C}_1\text{im}]\text{[PF}_6]$, $[\text{C}_7\text{C}_1\text{im}]\text{[PF}_6]$ and $[\text{C}_9\text{C}_1\text{im}]\text{[PF}_6]$. Some of the available data in literature for $[\text{C}_4\text{C}_1\text{im}]\text{[PF}_6]$, $[\text{C}_6\text{C}_1\text{im}]\text{[PF}_6]$ and $[\text{C}_8\text{C}_1\text{im}]\text{[PF}_6]$ presents a quite large uncertainty that in some cases exceed 10% [50, 83–87]. Only the available literature data with an uncertainty lower than 3% [23,75,82,88] was considered for data comparison. The volumic heat capacities, C_p^0/V , were calculated taking into account the specific heat capacities, c_p^0 , and the experimental density values at the same reference temperature reported in the literature [33]. Fig. 8 shows the graphic representation of the molar heat capacity data, $C_{p,m}^0$ and the specific heat capacity data, c_p^0 , at 298.15 K, as a function of the number of carbon atoms in the alkyl side chains of the cation, *n*, for the $[\text{C}_n\text{C}_1\text{im}]\text{[PF}_6]$ together with the literature data for the $[\text{C}_n\text{C}_1\text{im}]\text{[NTf}_2]$ ionic liquid series [38]. An apparent linearity behavior along the IL series is observed in the representation of $C_{p,m}^0$ (298.15 K) = $f(n)$ for the studied ILs.

At 298.15 K, the molar heat capacity of the $[\text{C}_n\text{C}_1\text{im}]\text{[NTf}_2]$ series is around $159 \text{ J K}^{-1} \text{ mol}^{-1}$ higher than those obtained for the $[\text{C}_n\text{C}_1\text{im}]\text{[PF}_6]$ series, which reflects the higher molar heat capacity contribution of the NTf_2 anion when compared with the PF_6 anion. The higher heat capacity contribution of the NTf_2 anion is due to the higher number of atoms (15 atoms) than the PF_6 anion (7 atoms), similar than the observed previously for the benzylimidazolium ionic liquids [12].

As it can be observed, the $[\text{C}_n\text{C}_1\text{im}]\text{[PF}_6]$ presents higher specific heat capacities than the bis triflamide based ILs. In addition, unlike to the trend shift found around $[\text{C}_6\text{C}_1\text{im}]\text{[NTf}_2]$ for $[\text{C}_n\text{C}_1\text{im}]\text{[NTf}_2]$ series [38], a subtle odd-even effect for the specific heat capacities, was found for the $[\text{C}_n\text{C}_1\text{im}]\text{[PF}_6]$, where the even numbered ILs presents higher c_p^0 . The observed odd-even effect in the heat capacity of the $[\text{C}_n\text{C}_1\text{im}]\text{[PF}_6]$ series could be rationalized considering a different preferential orientation of the terminal $-\text{CH}_3$ group in agreement than a similar effect observed previously [89] for the molar volume and molecular simulation

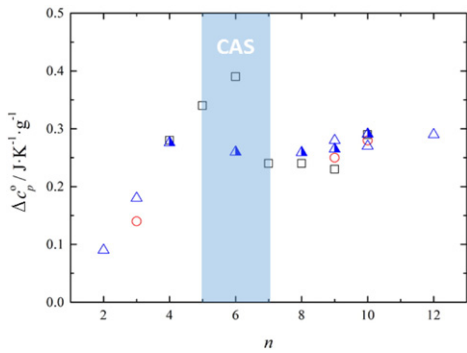


Fig. 5. Experimental specific heat capacity change, Δc_p associated to the phase transitions as a function of the number of carbons of the alkyl side chain of the cation, *n*, for $[\text{C}_n\text{C}_1\text{im}]\text{[PF}_6]$ (with *n* = 2–10, 12). This work: □, T_g ; ○, T_{cc} ; △, T_m ; ▲, Nemoto et al. [27].

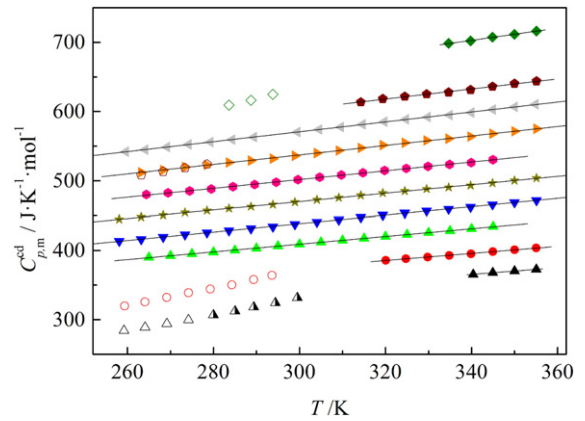


Fig. 6. Heat capacities of condensed phases $C_{p,mas}^{cd}$ as function of temperature, in the temperature range of 253–355 K. △ - C_2C_1 crystal phase 1; ▲ - C_2C_1 crystal phase 2; ▲ - C_2C_1 liquid phase; ○ - C_3C_1 crystal phase; ● - C_3C_1 liquid phase; ▲ - C_4C_1 liquid phase; ▼ - C_5C_1 liquid phase; ★ - C_6C_1 liquid phase; ● - C_7C_1 liquid phase; ▶ - C_8C_1 liquid phase; ◀ - C_9C_1 liquid phase; △ - C_{10}C_1 crystal phase; ● - C_{10}C_1 liquid phase; ◇ - C_{12}C_1 crystal phase; ◆ - C_{12}C_1 liquid phase.

showing that the cation side chains tend to adopt transoid conformations that pack head-to-head in the liquid phase. Fig. 9 presents the plot of the volumic heat capacity at 298.15 K as function of the number of carbon atoms in the alkyl side chain of the cation, *n*, and their comparison with the $[\text{C}_n\text{C}_1\text{im}]\text{[NTf}_2]$ [38].

The cation side chains tend to adopt transoid conformations that pack head-to-head in the liquid phase and in agreement with the previous work [89] in the $\text{C}_6\text{C}_1\text{im}$ cation series the even number tend to be less compact. The odd-even effect was already observed in some thermodynamic properties of different families of compounds, such as paraffin's [90], alcohols [91], fatty acids [92], and more recently in fluorotelomer alcohols [77,93] as well as in ILs [9,38,80,94]. However, it is still not clear why the sphericity and low charge dispersion of the hexafluorophosphate anion leads to a more pronounced odd-even effect on the heat capacities when compared with the bis triflamide anion. The observed subtle odd-even effect in the liquid phase is related with some preferential distribution of the chain tails in the apolar domain in agreement with the nanostructuration of the ILs [89]. The $[\text{C}_4\text{C}_1\text{im}]\text{[PF}_6]$ shows an outlier behavior from the trend of the homologous series, presenting a higher volumic heat capacity, in agreement with recent works reported in the literature for the short members of

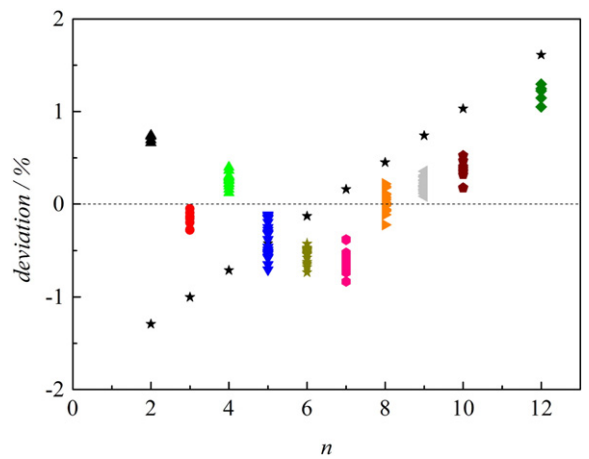


Fig. 7. Deviation from the linear model (Eq. (4)) of the experimental molar heat capacities of the liquid as function of “*n*” is number of carbons of the alkyl chain in the $[\text{C}_n\text{C}_1\text{im}]\text{[PF}_6]$ IL series (temperature range of 253–355 K). ▲ - C_2C_1 liquid phase; ● - C_3C_1 liquid phase; ▲ - C_4C_1 liquid phase; ▼ - C_5C_1 liquid phase; ★ - C_6C_1 liquid phase; ● - C_7C_1 liquid phase; ▶ - C_8C_1 liquid phase; ◀ - C_9C_1 liquid phase; △ - C_{10}C_1 liquid phase; ◆ - C_{12}C_1 liquid phase; ★ - deviation of the Gardas and Coutinho Model [81] at 298.15 K.

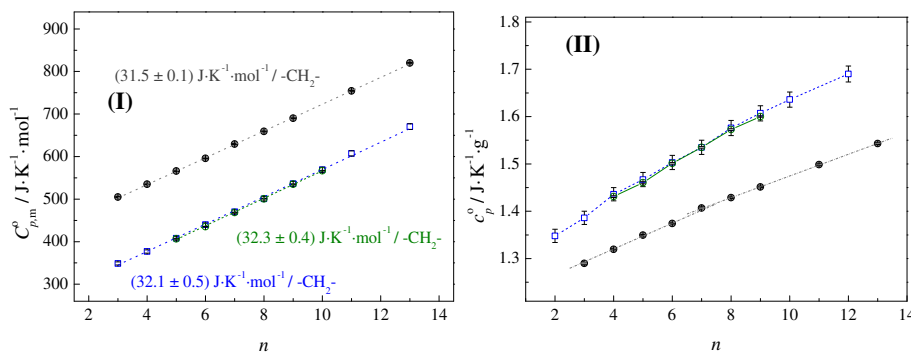


Fig. 8. Molar heat capacities (I) and specific heat capacities (II) at $T = 298.15\text{ K}$, as a function of the number of carbon atoms in the alkyl side chain of the cation n . \square - $[\text{C}_n\text{C}_1\text{im}]\text{[PF}_6]$ (with $n = 2\text{--}10, 12$), Setaram $\mu\text{DSC IIIa}$ microcalorimeter; \circ - $[\text{C}_n\text{C}_1\text{im}]\text{[PF}_6]$ (with $n = 5\text{--}10$), drop calorimeter; \bullet - $[\text{C}_n\text{C}_1\text{im}]\text{[NTf}_2]$ (with $n = 3\text{--}9, 11, 13$) [38].

the bistriflamide ILs series [38,95]. For a better understanding of the differentiation observed for the $[\text{C}_4\text{C}_1\text{im}]\text{[PF}_6]$, accurate data for the volumic heat capacity of the other short members of the series $[\text{C}_2\text{C}_1\text{im}]\text{[PF}_6]$ and $[\text{C}_3\text{C}_1\text{im}]\text{[PF}_6]$ (that are solids at 298.15 K), will be needed.

4. Final remarks

This work contributed to a better understanding of the complex thermal behavior of the ILs. Based on the obtained differences in the phase behavior, the studied series can be divided into three major groups: short, intermediate, and long alkyl chain members. For small alkyl chain members, as their size increases, the more difficult the packing mechanism is, explaining why the melting temperature starts to decrease. For the intermediate alkyl chain size members, the difficult packing system demands more energy to reach the crystalline phase, reflecting the increasing of T_{cc} . The $-\text{CH}_2-$ increments in shorts alkyl side chains, decreases the gap between electrostatic and dispersive interactions and this is observed in T_m . The T_m decreases per each $-\text{CH}_2-$ added, until it eventually intercepts T_{cc} , and no solid phase can be observed (intermediate region). The T_m of $[\text{C}_8\text{C}_1\text{im}]\text{[PF}_6]$ confirms this. The respective enthalpy and entropy showed that the melting was partially obtained due to the difficulty in the crystallization process. Many attempts were performed to achieve solid phase without success, with long isotherms (about a week) at 183 K were needed. For longer alkyl chains the packing mechanism is mainly controlled by dispersive interactions, leading to an easier packing of the alkyl chains and the increase of melting temperatures per $-\text{CH}_2-$ group added.

Polymorphism was observed in the region of short alkyl chains, in agreement with literature. This is the effect of the small alkyl chain and its easy rearrangement in the crystal structure, confirmed by the existence of solid-solid phase transitions with no well-defined temperature.

Besides the deviation that is expected from the intensification of the nanostructuration in the liquids phase after the so called CAS $n = 6$, a quite good linear dependence of the molar liquid heat capacities with (n and T), Eq. (4), for the $[\text{C}_n\text{C}_1\text{im}]\text{[PF}_6]$ IL series was found. The molar heat capacity of this series presents a linear increase with the number of the methylene groups in the alkyl chain (it increases about $32\text{ J K}^{-1}\text{ mol}^{-1}$ per methylene group at 298.15 K) and the specific heat capacities are dominated by the packing system and so, by the anion/cation interactions, where the $[\text{PF}_6]$ family presents higher values when compared with the $[\text{NTf}_2]$ (very large anion which hinders the packing system and with more dispersed electronegativity). The smaller size of $[\text{PF}_6]$ anion and the easiness in packing allows the detection of a subtle odd-even effect, result of the terminal $-\text{CH}_3$ group orientation.

Acknowledgements

Thanks are due to Fundação para a Ciência e Tecnologia (FCT - through the project SFRH/BD/94211/2013), Lisbon, Portugal and to FEDER for financial support to Centro de Investigação em Química, University of Porto through the project Pest-C/QUI/UI0081/2013 and NORTE-01-0145-FEDER-000028, Sustainable Advanced Materials (SAM). CICECO, University of Aveiro, through the project Pest-C/CTM/LA0011/2013. Paulo B. P. Serra acknowledges the financial support from specific university research (MSMT No. 20/2014). Filipe M. S. Ribeiro acknowledges the financial support from FCT and the European Social Fund (ESF) under the Community Support Framework (CSF) for the award of his Research Grants, SFRH/BD/94211/2013. The authors gratefully acknowledge a partial financial contribution from the COST (project CM1206 on “Exchange on Ionic Liquids”).

Appendix A. Supplementary data

Supplementary data to this article can be found online at <https://doi.org/10.1016/j.molliq.2017.10.042>.

References

- [1] M. Tariq, M.G. Freire, B. Saramago, J.A.P. Coutinho, J.N.C. Lopes, L.P.N. Rebelo, Surface tension of ionic liquids and ionic liquid solutions, *Chem. Soc. Rev.* 41 (2012) 829–868.
- [2] K. Paduszyński, U. Domańska, Viscosity of ionic liquids: an extensive database and a new group contribution model based on a feed-forward artificial neural network, *J. Chem. Inf. Model.* 54 (2014) 1311–1324.
- [3] S. Aparicio, M. Atilhan, F. Karadas, Thermophysical properties of pure ionic liquids: review of present situation, *Ind. Eng. Chem. Res.* 49 (2010) 9580–9595.
- [4] S. Zhang, N. Sun, X. He, X. Lu, X. Zhang, Physical properties of ionic liquids: database and evaluation, *J. Phys. Chem. Ref. Data* 35 (2006) 1475–1517.

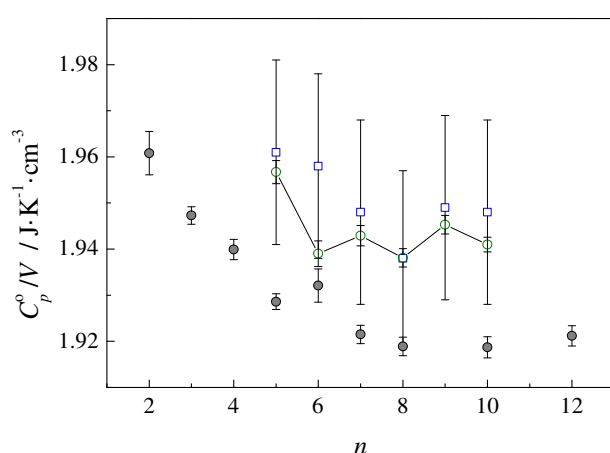


Fig. 9. Volumic heat capacities at $T = 298.15\text{ K}$, as a function of the number of carbon atoms in the alkyl side chains of the cation. \square - $[\text{C}_n\text{C}_1\text{im}]\text{[PF}_6]$ (with $n = 5\text{--}10$), $\mu\text{DSC IIIa}$; \circ - $[\text{C}_n\text{C}_1\text{im}]\text{[PF}_6]$ (with $n = 5\text{--}10$), drop calorimeter; \bullet - $[\text{C}_n\text{C}_1\text{im}]\text{[NTf}_2]$ (with $n = 2\text{--}8, 10, 12$) [38].

- [5] J.S.W. Wilkes, T. Welton, Ionic Liquids in Synthesis, Wiley-VCH Verlag GmbH & Co. KGaA, 2008 1–6.
- [6] K. Shimizu, M.F. Costa Gomes, A.A.H. Pádua, L.P.N. Rebelo, J.N. Canongia Lopes, Three commentaries on the nano-segregated structure of ionic liquids, *J. Mol. Struct. THEOCHEM* 946 (2010) 70–76.
- [7] A.S.M.C. Rodrigues, L.M.N.B.F. Santos, Nanostructuration effect on the thermal behaviour of ionic liquids, *ChemPhysChem* 17 (2016) 1512.
- [8] M. Vilas, M.A.A. Rocha, A.M. Fernandes, E. Tojo, L.M.N.B.F. Santos, Novel 2-alkyl-1-ethylpyridinium ionic liquids: synthesis, dissociation energies and volatility, *Phys. Chem. Chem. Phys.* 17 (2015) 2560–2572.
- [9] M.A.A. Rocha, C.F.R.A.C. Lima, L.R. Gomes, B. Schröder, J.A.P. Coutinho, I.M. Marrucho, J.M.S.S. Esperança, L.P.N. Rebelo, K. Shimizu, J.N.C. Lopes, L.M.N.B.F. Santos, High-accuracy vapor pressure data of the extended [CnClim][Ntf₂] ionic liquid series: trend changes and structural shifts, *J. Phys. Chem. B* 115 (2011) 10919–10926.
- [10] A.V. Blokhin, Y.U. Paulechka, A.A. Strechan, G.J. Kabo, Physicochemical properties, structure, and conformations of 1-butyl-3-methylimidazolium bis(trifluoromethanesulfonyl)imide [C4mim]Ntf₂ ionic liquid, *J. Phys. Chem. B* 112 (2008) 4357–4364.
- [11] J.D. Holbrey, W.M. Reichert, M. Nieuwenhuyzen, S. Johnson, K.R. Seddon, R.D. Rogers, Crystal polymorphism in 1-butyl-3-methylimidazolium halides: supporting ionic liquid formation by inhibition of crystallization, *Chem. Commun.* (2003) 1636–1637.
- [12] P.B.P. Serra, F.M.S. Ribeiro, M.A.A. Rocha, M. Fulém, K. Růžička, L.M.N.B.F. Santos, Phase Behavior and Heat Capacities of the 1-Benzyl-3-methylimidazolium Ionic Liquids, *J. Chem. Thermodyn.* 100 (2016) 124–130.
- [13] E.J. Donth, Description of the phenomenon, The Glass Transition: Relaxation Dynamics in Liquids and Disordered Materials, Springer, Berlin Heidelberg, Berlin, Heidelberg 2001, pp. 11–225.
- [14] P.L. Papon, J. Meijer, H.E. Paul, The Physics of Phase Transitions, Springer-Verlag Berlin Heidelberg, 2006.
- [15] C. Hardacre, J.D. Holbrey, P.B. McCormac, S.E.J. McMath, M. Nieuwenhuyzen, K.R. Seddon, Crystal and liquid crystalline polymorphism in 1-alkyl-3-methylimidazolium tetrachloropalladate(II) salts, *J. Mater. Chem.* 11 (2001) 346–350.
- [16] K. Nishikawa, S. Wang, H. Katayanagi, S. Hayashi, H.-o. Hamaguchi, Y. Koga, K.-i. Tozaki, Melting and freezing behaviors of prototype ionic liquids, 1-butyl-3-methylimidazolium bromide and its chloride, studied by using a Nano-watt differential scanning calorimeter, *J. Phys. Chem. B* 111 (2007) 4894–4900.
- [17] C.M. Gordon, J.D. Holbrey, A.R. Kennedy, K.R. Seddon, Ionic liquid crystals: hexafluorophosphate salts, *J. Mater. Chem.* 8 (1998) 2627–2636.
- [18] A. Triolo, A. Mandanici, O. Russina, V. Rodriguez-Mora, M. Cutroni, C. Hardacre, M. Nieuwenhuyzen, H.J. Bleif, L. Keller, M.A. Ramos, Thermodynamics, structure, and dynamics in room temperature ionic liquids: the case of 1-butyl-3-methylimidazolium hexafluorophosphate ([bmim][PF₆]), *J. Phys. Chem. B* 110 (2006) 21357–21364.
- [19] T. Endo, T. Morita, K. Nishikawa, Crystal polymorphism of a room-temperature ionic liquid, 1,3-dimethylimidazolium hexafluorophosphate: calorimetric and structural studies of two crystal phases having melting points of ~50 K difference, *Chem. Phys. Lett.* 517 (2011) 162–165.
- [20] T. Endo, K. Nishikawa, Thermal phase behavior of 1-butyl-3-methylimidazolium hexafluorophosphate: simultaneous measurements of the melting of two polymorphic crystals by Raman spectroscopy and calorimetry, *Chem. Phys. Lett.* 584 (2013) 79–82.
- [21] T. Endo, T. Kato, K. Tozaki, K. Nishikawa, Phase behaviors of room temperature ionic liquid linked with cation conformational changes: 1-butyl-3-methylimidazolium hexafluorophosphate, *J. Phys. Chem. B* 114 (2010) 407–411.
- [22] M.A.A. Rocha, C.M.S.S. Neves, M.G. Freire, O. Russina, A. Triolo, J.A.P. Coutinho, L.M.N.B.F. Santos, Alkylimidazolium based ionic liquids: impact of cation symmetry on their nanoscale structural organization, *J. Phys. Chem. B* 117 (2013) 10889–10897.
- [23] G.J. Kabo, A.V. Blokhin, Y.U. Paulechka, A.G. Kabo, M.P. Shymanovich, J.W. Magee, Thermodynamic properties of 1-butyl-3-methylimidazolium hexafluorophosphate in the condensed state, *J. Chem. Eng. Data* 49 (2004) 453–461.
- [24] J.D. Holbrey, K.R. Seddon, The phase behaviour of 1-alkyl-3-methylimidazolium tetrafluoroborates; ionic liquids and ionic liquid crystals, *J. Chem. Soc. Dalton Trans.* (1999) 2133–2140.
- [25] S.V. Dzyuba, R.A. Bartsch, Influence of structural variations in 1-alkyl(aralkyl)-3-methylimidazolium hexafluorophosphates and bis(trifluoromethylsulfonyl)imides on physical properties of the ionic liquids, *ChemPhysChem* 3 (2002) 161–166.
- [26] Y. Zhang, E.J. Maginn, Molecular dynamics study of the effect of alkyl chain length on melting points of [CnMIM][PF₆] ionic liquids, *Phys. Chem. Chem. Phys.* 16 (2014) 13489–13499.
- [27] F. Nemoto, M. Kofu, O. Yamamoto, Thermal and structural studies of imidazolium-based ionic liquids with and without liquid-crystalline phases: the origin of nanostructure, *J. Phys. Chem. B* 119 (2015) 5028–5034.
- [28] Y. Shimizu, Y. Ohte, Y. Yamamura, K. Saito, Is the liquid or the solid phase responsible for the low melting points of ionic liquids? Alkyl-chain-length dependence of thermodynamic properties of [CnMIM][NTf₂], *Chem. Phys. Lett.* 470 (2009) 295–299.
- [29] J. Konicek, I. Wadsö, J. Suurkuus, Precise drop heat-capacity calorimeter for small samples, *Chem Scripta* 1 (1971) 217–&.
- [30] J. Suurkuus, I. Wadsö, Design and testing of an improved precise drop calorimeter for the measurement of the heat capacity of small samples, *J. Chem. Thermodyn.* 6 (1974) 667–679.
- [31] L.M.N.B.F. Santos, M.A.A. Rocha, A.S.M.C. Rodrigues, V. Štejfa, M. Fulém, M. Bastos, Reassembling and testing of a high-precision heat capacity drop calorimeter. Heat capacity of some polyphenyls at T = 298.15 K, *J. Chem. Thermodyn.* 43 (2011) 1818–1823.
- [32] M.A.A. Rocha, J.A.P. Coutinho, L.M.N.B.F. Santos, Evidence of nanostructuration from the heat capacities of the 1,3-dialkylimidazolium bis(trifluoromethylsulfonyl)imide ionic liquid series, *J. Chem. Phys.* 139 (2013) 104502.
- [33] M.A.A. Rocha, F.M.S. Ribeiro, A.I.M.C.L. Ferreira, J.A.P. Coutinho, L.M.N.B.F. Santos, Thermophysical properties of [CN – C1Clm][PF₆] ionic liquids, *J. Mol. Liq.* 188 (2013) 196–202.
- [34] M.A.A. Rocha, J.A.P. Coutinho, L.M.N.B.F. Santos, Cation symmetry effect on the volatility of ionic liquids, *J. Phys. Chem. B* 116 (2012) 10922–10927.
- [35] G.W.H. Höhne, W. Hemminger, H.-J. Flammersheim, Differential Scanning Calorimetry: An Introduction for Practitioners, Springer, Berlin Heidelberg, Berlin, Heidelberg, 1996 1–6.
- [36] M. Straka, K. Růžička, V. Růžička, Heat capacities of chloroanilines and chloronitrobenzenes, *J. Chem. Eng. Data* 52 (2007) 1375–1380.
- [37] M. Fulém, V. Laštovka, M. Straka, K. Růžička, J.M. Shaw, Heat capacities of tetracene and pentacene, *J. Chem. Eng. Data* 53 (2008) 2175–2181.
- [38] M.A.A. Rocha, M. Bastos, J.A.P. Coutinho, L.M.N.B.F. Santos, Heat capacities at 298.15 K of the extended [CnClm][Ntf₂] ionic liquid series, *J. Chem. Thermodyn.* 53 (2012) 140–143.
- [39] M.A.A. Rocha, J.A.P. Coutinho, L.M.N.B.F. Santos, Vapor pressures of 1,3-dialkylimidazolium bis(trifluoromethylsulfonyl)imide ionic liquids with long alkyl chains, *J. Chem. Phys.* 141 (2014) 134502.
- [40] E.S.B. Carlos, M.N.B.F. Luís, E.M.D.P. Manuel, A new calorimetric system to measure heat capacities of solids by the drop method, *Meas. Sci. Technol.* 17 (2006) 1405.
- [41] R. Sabah, A. Xu-wu, J.S. Chickos, M.L.P. Leitão, M.V. Roux, L.A. Torres, Reference materials for calorimetry and differential thermal analysis, *Thermochim. Acta* 331 (1999) 93–204.
- [42] V.D. Robert, D. Chirico, Joseph W. Magee, Michael Frenkel, Kenneth N. Marsh, Thermodynamics and thermophysical properties of the reference ionic liquid: 1-hexyl-3-methylimidazolium bis[(trifluoromethyl)sulfonyl]amide (including mixtures). Part 2. Critical evaluation and recommended property values, *Pure Appl. Chem.* 81 (2009) 791–828.
- [43] M.E. Wieser, M. Berglund, Atomic weights of the elements 2007 (IUPAC technical report), *Pure Appl. Chem.* 81 (2009) 2131–2156.
- [44] J. Vila, B. Fernández-Castro, E. Rilo, J. Carrete, M. Domínguez-Pérez, J.R. Rodríguez, M. García, L.M. Varela, O. Cabeza, Liquid-solid-liquid phase transition hysteresis loops in the ionic conductivity of ten imidazolium-based ionic liquids, *Fluid Phase Equilib.* 320 (2012) 1–10.
- [45] U. Domańska, A. Marciniak, Solubility of 1-alkyl-3-methylimidazolium hexafluorophosphate in hydrocarbons, *J. Chem. Eng. Data* 48 (2003) 451–456.
- [46] H. Sifaoui, A. Ait-Kaci, A. Modarressi, M. Rogalski, Solid-liquid equilibria of three binary systems: {1-ethyl-3-methylimidazolium hexafluorophosphate + 2-phenylimidazole, or 4,5-diphenylimidazole or 2,4,5-triphenylimidazole}, *Thermochim. Acta* 456 (2007) 114–119.
- [47] H.L. Ngo, K. LeCompte, L. Hargens, A.B. McEwen, Thermal properties of imidazolium ionic liquids, *Thermochim. Acta*, 357–358 (2000) 97–102.
- [48] D.S.H. Wong, J.P. Chen, J.M. Chang, C.H. Chou, Phase equilibria of water and ionic liquids [emim][PF₆] and [bmim][PF₆], *Fluid Phase Equilib.*, 194–197 (2002) 1089–1095.
- [49] H. Tokuda, S. Tsuzuki, M.A.B.H. Susan, K. Hayamizu, M. Watanabe, How ionic are room-temperature ionic liquids? An indicator of the physicochemical properties, *J. Phys. Chem. B* 110 (2006) 19593–19600.
- [50] C.P. Fredlake, J.M. Crosthwaite, D.G. Hert, S.N.V.K. Aki, J.F. Brennecke, Thermophysical properties of imidazolium-based ionic liquids, *J. Chem. Eng. Data* 49 (2004) 954–964.
- [51] J.G. Huddleston, A.E. Visser, W.M. Reichert, H.D. Willauer, G.A. Broker, R.D. Rogers, Characterization and comparison of hydrophilic and hydrophobic room temperature ionic liquids incorporating the imidazolium cation, *Green Chem.* 3 (2001) 156–164.
- [52] Z.H. Zhang, T. Cui, J.L. Zhang, H. Xiong, G.P. Li, L.X. Sun, F. Xu, Z. Cao, F. Li, J.J. Zhao, Thermodynamic investigation of room temperature ionic liquid, *J. Therm. Anal. Calorim.* 101 (2009) 1143–1148.
- [53] E.R. Talaty, S. Raja, V.J. Storhaug, A. Dölle, W.R. Carper, Raman and infrared spectra and ab initio calculations of C2-4MIM imidazolium hexafluorophosphate ionic liquids, *J. Phys. Chem. B* 108 (2004) 13177–13184.
- [54] V. Strehmel, A. Laschewsky, H. Krudelt, H. Wetzel, E. Görnitz, Free radical polymerization of methacrylates in ionic liquids, in: ionic liquids in polymer systems, Am. Chem. Soc. (2005) 17–36.
- [55] S.M. Urahata, M.C.C. Ribeiro, Single particle dynamics in ionic liquids of 1-alkyl-3-methylimidazolium cations, *J. Chem. Phys.* 122 (2005), 024511.
- [56] N. Shamim, G.B. McKenna, Glass dynamics and anomalous aging in a family of ionic liquids above the glass transition temperature, *J. Phys. Chem. B* 114 (2010) 15742–15752.
- [57] L.C. Branco, J.N. Rosa, J.J. Moura Ramos, C.A.M. Afonso, Preparation and characterization of new room temperature ionic liquids, *Chem. Eur. J.* 8 (2002) 3671–3677.
- [58] W. Xu, E.I. Cooper, C.A. Angell, Ionic liquids: ion mobilities, glass temperatures, and fragilities, *J. Phys. Chem. B* 107 (2003) 6170–6178.
- [59] S. Holopainen, M. Nousiainen, J. Puton, M. Sillanpää, U. Bardi, A. Tolstogouzov, Evaporation of ionic liquids at atmospheric pressure: study by ion mobility spectrometry, *Talanta* 83 (2011) 907–915.
- [60] J. Flieger, A. Czajkowska-Želazko, Identification of ionic liquid components by RP-HPLC with diode array detector using chaotropic effect and perturbation technique, *J. Sep. Sci.* 35 (2012) 248–255.
- [61] B.M. Su, S. Zhang, Z.C. Zhang, Structural elucidation of thiophene interaction with ionic liquids by multinuclear NMR spectroscopy, *J. Phys. Chem. B* 108 (2004) 19510–19517.

- [62] N.V. Plechkova, K.R. Seddon, Ionic Liquids Completely Uncoiled: Critical Expert Overviews, 2015.
- [63] Y.U. Paulechka, A.V. Blokhin, G.J. Kabo, A.A. Strechan, Thermodynamic properties and polymorphism of 1-alkyl-3-methylimidazolium bis(triflamides), *J. Chem. Thermodyn.* 39 (2007) 866–877.
- [64] C. Guerrero-Sánchez, T. Lara-Ceniceros, E. Jimenez-Regalado, M. Raşa, U.S. Schubert, Magnetorheological fluids based on ionic liquids, *Adv. Mater.* 19 (2007) 1740–1747.
- [65] C. Červinka, A.A.H. Pádua, M. Fulem, Thermodynamic properties of selected homologous series of ionic liquids calculated using molecular dynamics, *J. Phys. Chem. B* 120 (2016) 2362–2371.
- [66] E.S. Domalski, E.D. Hearing, Heat capacities and entropies of organic compounds in the condensed phase volume II, *J. Phys. Chem. Ref. Data* 19 (1990) 881–1047.
- [67] A.A. Schaerer, C.J. Busso, A.E. Smith, L.B. Skinner, Properties of pure normal alkanes in the C17 to C36 range, *J. Am. Chem. Soc.* 77 (1955) 2017–2019.
- [68] H.L. Finke, M.E. Gross, G. Waddington, H.M. Huffman, Low-temperature thermal data for the nine normal paraffin hydrocarbons from octane to hexadecane, *J. Am. Chem. Soc.* 76 (1954) 333–341.
- [69] R.C.F. Schaake, J.C.A. Offringa, G.J.K. van der Berg, J.C. van Miltenburg, Phase transitions in solids, studied by adiabatic calorimetry. I. Design and test of an automatic adiabatic calorimeter, *Recl. Trav. Chim. Pays-Bas* 98 (1979) 408–412.
- [70] J.F. Messerly, G.B. Guthrie, S.S. Todd, H.L. Finke, Low-temperature thermal data for pentane, n-heptadecane, and n-octadecane. Revised thermodynamic functions for the n-alkanes, C5–C18, *J. Chem. Eng. Data* 12 (1967) 338–346.
- [71] E.S. Domalski, E.D. Hearing, Heat capacities and entropies of organic compounds in the condensed phase. Volume III, *J. Phys. Chem. Ref. Data* 25 (1996) 1–525.
- [72] V.M. Lantsov, A.I. Maklakov, M.R. Zaripov, L.Y. Chenborisova, G.M. Kadievskii, Study of the motion of alkyl chains in plasticizers by the impulse method of nuclear magnetic resonance, *Polym. Sci. U.S.S.R.* 11 (1969) 2703–2709.
- [73] J.D. Kemp, C.J. Egan, Hindered rotation of the methyl groups in propane. The heat capacity, vapor pressure, heats of fusion and vaporization of propane. entropy and density of the gas, *J. Am. Chem. Soc.* 60 (1938) 1521–1525.
- [74] I. López-Martin, E. Burello, P.N. Davey, K.R. Seddon, G. Rothenberg, Anion and cation effects on imidazolium salt melting points: a descriptor modelling study, *ChemPhysChem* 8 (2007) 690–695.
- [75] J. Troncoso, C.A. Cerdeirinha, Y.A. Sanmamed, L. Romani, L.P.N. Rebelo, Thermodynamic properties of imidazolium-based ionic liquids: densities, heat capacities, and enthalpies of fusion of [bmim][PF6] and [bmim][NTf2], *J. Chem. Eng. Data* 51 (2006) 1856–1859.
- [76] A.T. Balaban, D.J. Klein, N.H. March, M.P. Tosi, M. Ausloos, Phase-transition regularities in critical constants, fusion temperatures and enthalpies of chemically similar chainlike structures, *ChemPhysChem* 6 (2005) 1741–1745.
- [77] J.C.S. Costa, M. Fulem, B. Schröder, J.A.P. Coutinho, M.J.S. Monte, L.M.N.B.F. Santos, Evidence of an odd–even effect on the thermodynamic parameters of odd fluorotelomer alcohols, *J. Chem. Thermodyn.* 54 (2012) 171–178.
- [78] E. Badea, B. Nowicka, G. Della Gatta, Thermodynamics of fusion and sublimation for a homologous series of eleven alkane- α,ω -diols HO-(CH₂)_n-OH: structure-related odd–even effect, *J. Chem. Thermodyn.* 68 (2014) 90–97.
- [79] J.N.A. Canongia Lopes, A.A.H. Pádua, Nanostructural organization in ionic liquids, *J. Phys. Chem. B* 110 (2006) 3330–3335.
- [80] W. Zheng, A. Mohammed, L.G. Hines, D. Xiao, O.J. Martinez, R.A. Bartsch, S.L. Simon, O. Russina, A. Triolo, E.L. Quitevis, Effect of cation symmetry on the morphology and physicochemical properties of imidazolium ionic liquids, *J. Phys. Chem. B* 115 (2011) 6572–6584.
- [81] R.L. Gardas, J.A.P. Coutinho, A group contribution method for heat capacity estimation of ionic liquids, *Ind. Eng. Chem. Res.* 47 (2008) 5751–5757.
- [82] C.A. Nieto de Castro, M.J.V. Lourenço, A.P.C. Ribeiro, E. Langa, S.I.C. Vieira, P. Goodrich, C. Hardacre, Thermal properties of ionic liquids and ionanofluids of imidazolium and pyrrolidinium liquids, *J. Chem. Eng. Data* 55 (2010) 653–661.
- [83] Y.H. Yu, A.N. Soriano, M.-H. Li, Heat capacities and electrical conductivities of 1-n-butyl-3-methylimidazolium-based ionic liquids, *Thermochim. Acta* 482 (2009) 42–48.
- [84] Y.H. Yu, A.N. Soriano, M.-H. Li, Heat capacity and electrical conductivity of aqueous mixtures of [Bmim][BF4] and [Bmim][PF6], *J. Taiwan Inst. Chem. Eng.* 40 (2009) 205–212.
- [85] J.G. Li, Y.F. Hu, S. Ling, J.-Z. Zhang, Physicochemical properties of [C6mim][PF6] and [C6mim][(C2F5)3PF3] ionic liquids, *J. Chem. Eng. Data* 56 (2011) 3068–3072.
- [86] J.D. Holbrey, W.M. Reichert, R.G. Reddy, R.D. Rogers, Heat capacities of ionic liquids and their applications as thermal fluids, *ACS Symp. Ser.* 856 (2003) 121–133.
- [87] E.E. Zvereva, S.A. Katsyuba, P.J. Dyson, A simple physical model for the simultaneous rationalisation of melting points and heat capacities of ionic liquids, *Phys. Chem. Chem. Phys.* 12 (2010) 13780–13787.
- [88] Y.U. Paulechka, Heat capacity of room-temperature ionic liquids: a critical review, *J. Phys. Chem. Ref. Data* 39 (2010).
- [89] G. Adamova, L. P. N. Rebelo, K. Shimizu, J. N. Canongia Lopes, Luis M. N. B. F. Santos, K. Seddon, The alternation effect in ionic liquid homologous series *Phys. Chem. Chem. Phys.*, 16 (2014) 4033–4038.
- [90] G.R. Somayajulu, The melting-points of ultralong paraffins and their homologs, *Int. J. Thermophys.* 11 (1990) 555–572.
- [91] H. Izumi, S. Yamagami, S. Futamura, L.A. Nafie, R.K. Dukor, Direct observation of odd – even effect for chiral alkyl alcohols in solution using vibrational circular dichroism spectroscopy, *J. Am. Chem. Soc.* 126 (2004) 194–198.
- [92] D.G. Yablon, D. Wintgens, G.W. Flynn, Odd/even effect in self-assembly of chiral molecules at the liquid – solid interface: an STM investigation of coadsorbate control of self-assembly, *J. Phys. Chem. B* 106 (2002) 5470–5475.
- [93] M. Fulem, K. Růžička, C. Červinka, A. Bazyleva, G. Della Gatta, Thermodynamic study of alkane- α,ω -diamines – evidence of odd–even pattern of sublimation properties, *Fluid Phase Equilib.* 371 (2014) 93–105.
- [94] G. Adamova, R.L. Gardas, L.P.N. Rebelo, A.J. Robertson, K.R. Seddon, Alkyldioctylphosphonium chloride ionic liquids: synthesis and physicochemical properties, *Dalton Trans.* 40 (2011) 12750–12764.
- [95] M.A.A. Rocha, F.M.S. Ribeiro, B. Schröder, J.A.P. Coutinho, L.M.N.B.F. Santos, Volatility study of [C1Clim][NTf2] and [C2C3im][NTf2] ionic liquids, *J. Chem. Thermodyn.* 68 (2014) 317–321.